SECOND EUROPEAN CONFERENCE ON EARTHQUAKE ENGINEERING
AND SEISMOLOGY, ISTANBUL AUG. 25-29, 2014

IMPLICATIONS OF EARTHQUAKE RECURRENCE MODELS TO THE SEISMIC HAZARD ESTIMATES IN THE MARMARA REGION, TURKEY

Aybige AKINCI[1], Maura MURRU[1], Rodolfo CONSOLE[2], Giuseppe FALCONE[1], Stefano PUCCI[1]

ABSTRACT

In this study, we show the effect of time-independent and time-dependent occurrence models on the seismic hazard estimations. The time-dependency is introduced by 1) the Brownian Passage Time (BPT) probability model that is based on a simple physical model of the earthquake cycle 2) the fusion of the BPT renewal model (BPT+Δ*CFF*) with a physical model that considers the earthquake probability perturbation for interacting faults by static Coulomb stress changes. To do so, we calculate the probability of occurrence of earthquakes $M_w > 6.5$ for individual fault sources in the Marmara region for the 5-10-30 and 50-year periods (starting from January 1, 2013). We treat the uncertainties in the fault parameters (e.g. slip rate, characteristic magnitude and aperiodicity) of the statistical distribution associated to each examined fault source by a Monte Carlo technique. Then the probabilities of occurrence for the next characteristic earthquake are calculated from three different models (Poisson, BPT, and BPT+Δ*CFF*) considering the 10^{th}, 50^{th} and 90^{th} percentiles of the Monte Carlo distribution.

In order to evaluate the impact of the earthquake probability models to ground motion hazard we attempt to calculate the fault-based probabilistic seismic hazard maps (PSHA) of mean Peak Ground Acceleration (PGA) having 10% probability of exceedance in 50 years on rock site condition. We note that in the present study we did not take in to account the ground motion variability caused by the different GMPE choices. In fact only one GMPE model is chosen as defined by Akkar and Cagnan (2010) (hereafter, AC10) for the active shallow crustal region for assessing the ground shaking hazard in the Marmara region in order to avoid those variability's effect the final seismic hazard estimations in the study region.

We observed that the impact of the different occurrence models on the seismic hazard estimate of selected sites is quite high: the hazard may increase by more than 70% or decrease by as much as 70%, depending on the applied model. We demonstrated that the estimated average recurrence time and the associated magnitude together with the elapsed time are crucial parameters in the earthquake probability calculations.

[1] Implications of Earthquake Recurrence Models to the Seismic Hazard Estimates in the Marmara Region, Turkey, INGV, Roma1, Rome, aybige.akinci@ingv.it, maura.murru@ingv.it, giuseppe.falcone@ingv.it, stefano.pucci@ingv.it

[2] Implications of Earthquake Recurrence Models to the Seismic Hazard Estimates in the Marmara Region, Turkey, Center of Integrated Geomorphology for the Mediterranean Area, Potenza.

INTRODUCTION

Recent studies confirm that present-day loading, slip deficit and thus seismic hazard appear to be particularly high along the segments located in the Marmara Sea, southwest of Istanbul (Armijo et al. 2005; Pondard et al., 2007). As a consequence of stress transfer due to the August 17, 1999 M_w7.4 Izmit earthquake another large and destructive earthquake is now expected to occur further west along the North Anatolian fault to strike Istanbul with a probability of strong shaking of 62±15% over the next 30 years (Parson et al., 2000). Because of the real earthquake threat in the Marmara region, the need for seismic hazard studies has become progressively more important (Atakan et al., 2002; Erdik et al., 2004; Kalkan et al., 2005; Gulerce and Ocak, 2013).

The objective of this study is to evaluate the uncertainty in the earthquake hazard related to the uncertainty in the geologic information and the impact of the different earthquake occurrence models to the seismic hazard in the Marmara Region using a PSHA methodology. The consideration of epistemic uncertainties serves both to quantify the range of seismic hazard for a given exceedance probability and also importantly to illustrate which model assumptions lead to the most significant variation in the estimated hazard.

Based on recent geological and seismological findings available in literature, first of all, we develop a fault segmentation model as shown in Figure 1. The first step to build this model was to define the geometry of the fault system of each NAFZ branches on the basis of its structural arrangement. The fault system is reconstructed at both surface and depth. In particular, the reconstruction of the fault traces at the surface benefits of the recognition of the surface ruptures produced by recent earthquakes (e.g. 1999, 1912, and 1894). In the second step we define fault segments as those faults that are supposed to be bounded by permanent barriers. We analyzed the possible factors of the fault system able to act as potential, permanent barriers to rupture propagation. These factors are those controlling rupture propagation in terms of pure geometric fault complexities (e.g. jogs and fault-bends) (Segall and Pollard, 1980; Barka and Kandisky-Cade, 1988; Wesnousky, 1988; Lettis et al., 2002; An, 1997), of rupture dynamics (Sibson, 1985; Harris and Day, 1999; Kase and Kuge, 2001), or in terms of behavioural characteristics. Such well-constrained data integration is necessary to compute more realistic scenarios of ground acceleration on the Marmara region and, in turn, of the basis for future models of seismic hazard assessment.

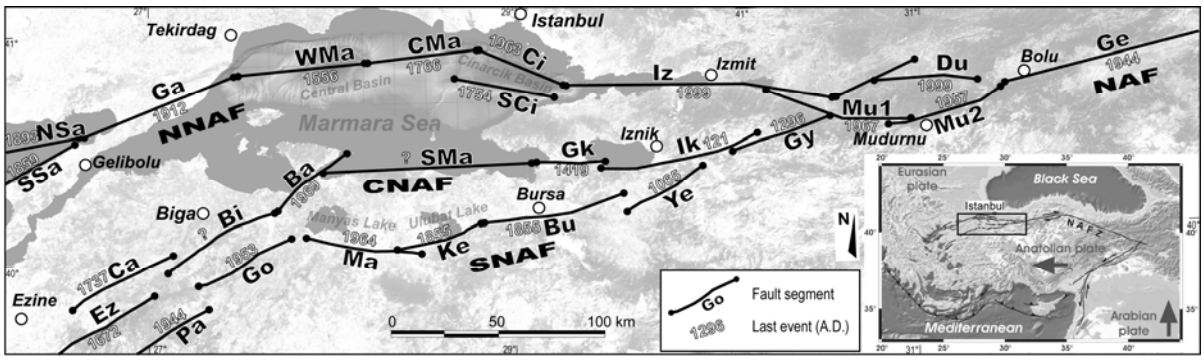

Figure 1 Fault segmentation model for the Marmara region.

Earthquake recurrence rates are calculated assuming the characteristic earthquake model for the events $M_w > 6.5$. The return periods estimated are based on the slip rate hypotheses, which were derived from Table 1. In fact, the recurrence time (T_r) is the basic ingredient to compute earthquake probability, both under time-independent, Poissonian assumption and in time-dependent, renewal approaches. It is the recurrence intervals or inter-event time between similar-sized, maximum expected earthquakes on the individual source. Since we do not have multiple characteristic events associated to the same fault segment the value of T_r has to be derived by the combination of fault rupture parameters. We invoke the criterion of "segment total seismic moment rate conservation", proposed by Field et al. (1999) allowing multi-segments ruptures.

Table 1. Fault parameters used in the modeling: kinematics (SS=strike-slip; N=normal); slip rate (SR);dip angle (Dip); length (L); depth (H); width (W); last event age; Maximum expected magnitude (*M*), computed by instrumental or historical data; otherwise by fault geometry (Wells and Coppersmith, 1994); penultimate event.

#	Fault name	Kin	M_w	Slip Rate (mm/yr)	L (km)	H (km)	W (km)	strike (°)	dip (°)	rake (°)	Last Event (AD)	Penultimate Event (AD)	T-elapsed
1	Izmit	SS	7.4±0.2	15±3.0	158	15	15.08	271	84	185	17/08/1999	03/05/1874	14
2	Cinarcik	N	7.0±0.2	12±2.4	44	15	16.55	116	65	205	10/07/1894	-	119
3	South Cinarcik	N	6.8±0.2	3±0.6	48	15	16.55	283	65	205	02/09/1754	-	259
4	Central Marmara	SS	7.2±0.2	15±3.0	49	15	15.08	83	84	185	22/05/1766	10/09/1509	247
5	West Marmara	SS	7.2±0.3	15±3.0	61	15	15.34	84	78	190	10/05/1556	-	457
6	Ganos	SS	7.4±0.2	18±3.5	74	15	15..53	246	75	177	09/08/1912	05/08/1766	101
7	North Saros	SS	7.1±0.2	9±0.8	46	15	15.96	76	70	194	09/02/1893	17/02/1659	120
8	South Saros	SS	7.1±0.2	9±0.8	45	15	15.53	241	75	194	21/08/1859	18/05/1625	154
9	Mudurnu	SS	7.2±0.2	10±2.0	70	15	15.06	291	85	185	22/07/1967	25/05/1719	46
10	Abant	SS	7.2±0.2	10±2.0	55	15	15.34	236	78	183	26/05/1957	17/08/1668	56
11	Duzce	SS	7.1±0.2	15±3.0	42	15	15.67	276	73	183	12/11/1999	19/04/1878	14
12	Gerede	SS	7.5±0.2	15±3.0	165	15	15.06	261	85	10	01/02/1944	17/08/1668	69
13	Geyve	SS	7.0±0.3	5±1.0	49	15	15.34	256	78	200	01/06/1296	-	717
14	Iznik	SS	7.4±0.3	3±0.6	74	15	15.34	259	78	200	01/01/121	-	1892
15	Yenisehir	SS	6.8±0.3	2±0.4	40	15	15.34	237	78	200	01/09/1065	-	948
16	Gemlik	N	6.8±0.2	3±0.6	30	15	19.58	271	50	250	11/04/1855	15/03/1419	158
17	Bursa	SS	6.8±0.2	3±0.6	67	15	15.23	261	80	200	19/04/1850	-	163
18	South Marmara	N	7.1±0.3	2±0.4	96	15	19.58	268	50	258	10/05/1556	-	457
19	Kemalpasa	SS	7.4±0.2	3±0.6	41	15	15.34	254	78	190	28/02/1855	-	158
20	Manyas	N	6.9±0.2	6±1.2	55	15	19.58	282	50	258	10/06/1964	-	49
21	Bandirma	N	7.0±0.3	3±0.6	41	15	19.58	231	50	200	10/11/123	-	1890
22	Gonen	SS	7.1±0.2	4±0.8	50	15	15.96	243	70	180	18/03/1953	-	60
23	Biga	SS	7.0±0.2	3±0.6	57	15	15.96	241	70	180	03/03/1969	-	44
24	Pazarkoy	N	6.8±0.2	2±0.4	54	15	19.58	60	50	240	01/02/1944	-	69
25	Can	SS	7.0±0.2	3±0.6	53	15	15.96	241	70	180	06/03/1737	-	276
26	Ezine	SS	7.0±0.2	2±0.4	56	15	15.96	238	70	180	08/02/1826	14/02/1672	187

EARTHQUAKE RECURRENCE MODELS

We then use three probability models to represent the recurrence time probability distribution for earthquakes on single sources: the time-independent Poisson model, time-dependent BPT model and one based on the BPT distribution including the permanent effect of the stress interaction among faults. For a uniform Poisson model the expected recurrence time T_r is the only necessary piece of information. Its earthquake hazard is constant in time and the probability density function (pdf) is a negative exponential function:

$$f(t) = \frac{1}{T_r} \exp\left\{-\frac{t}{T_r}\right\} \quad (1)$$

where t is the elapsed time since the latest characteristic earthquake, and T_r is the mean inter-event time.

For the BPT distribution, also known as the inverse Gaussian distribution, the hazard function (e.g. the instantaneous value of the conditional rate density) starts from zero soon after an event, it increases as the elapsed time from the last characteristic event approaches the recurrence time, and then is asymptotic to some constant level for elapsed times much larger than the average elapsed time. The pdf (Matthews et al., 2002) is given by:

$$f(t;T_r,\alpha) = \left(\frac{T_r}{2\pi\alpha^2 t^3}\right)^{1/2} \exp\left\{-\frac{(t-T_r)^2}{2T_r\alpha^2 t}\right\} \quad (2)$$

where t is the elapsed time from the last characteristic event and α, dimensionless measure, is the coefficient of variation (also known as the aperiodicity) of the distribution. The aperiodicity parameter describes how regularly or irregularly characteristic earthquakes are expected to occur on any time-dependent fault. This parameter is ordinarily derived from the coefficient of variation of actual observed recurrence time intervals on individual faults and can be reinforced with geological evidence (Ellsworth et al., 1999; Cramer et al., 2000). This variation coefficient is given by the ratio of the standard deviation of inter-event times between large events that rupture all or most of a given fault segment over the mean recurrence time for that segment. The smaller are α values, the higher is the probability of occurrence for elapsed times long compared to the mean recurrence time. On the other hand, as the α value increases and approaches unity, the process becomes less strongly quasi-periodic and becomes increasingly Poisson like. It is a key parameter in time-varying probability calculations. In this study, in the absence of any statistical assessment, due to the low number of events reported on each segment, we have considered for the variability of the aperiodicity a range from 0.3 to 0.7.
The time-dependent probability calculation follows the renewal hypothesis of earthquake regeneration such that earthquake likelihood on a fault is lowest just after the last event. As tectonic stress grows, the odds of another earthquake increase. In fact, according to the theory of elasticity, the co-seismic slip of an earthquake associated with a certain fault segment results in a redistribution of the stress in the surrounding crustal volume. The interaction is taken into consideration by the computation of the Coulomb static stress change, as the Coulomb Failure Function change (ΔCFF), caused by previous earthquakes on the concerned fault (King et al., 1994). The stress change ΔCFF on an individual fault is computed adding the contributions from all the other sources that have ruptured after the latest known earthquake on the considered fault. The computation is carried out all over the source area. The algorithm for ΔCFF calculation assumes an Earth model such as a half space characterized by uniform elastic properties. For calculating the Coulomb Failure Function, the knowledge of the fault parameters of the causative and the receiving sources, as well as the focal mechanism (strike, dip, and rake), dimensions (width and length) and average slip for all the triggering earthquakes is necessary. In absence of direct information about the slip distribution for the causative earthquakes considered in this study, we have assumed for all of them a distribution consistent with a uniform stress drop on the rectangle of the segment fault. We have calculated the slip distribution that satisfies the condition of zero slip on the edge and maximum at the center on the rectangle of the causative source (Console et al., 2008 and 2013). The calculation is carried out for each node of a dense rectangular grid. The maximum value of the slip is defined through the relation

$$\Delta_{\mathrm{umax}} = \frac{16}{\pi^2}\frac{\mathrm{M_0}}{\mu \mathrm{WL}} \qquad (3)$$

where μ is the shear modulus (rigidity) of the elastic medium, W and L the dimensions of the causative fault and M_0 is the seismic moment derived from the Kanamori and Anderson (1975) relation.

The effective friction coefficient adopted in this study is 0.4, which is closer to friction value for major faults (Harris and Simpson, 1998). The effect of ΔCFF on the probability for the future characteristic earthquakes assumes that the time elapsed since the previous earthquake is modified from t to t' by a shift, Δt, proportional to ΔCFF, that is

$$t' = t + \Delta t = t + (\Delta CFF / \tau) \qquad (4)$$

where τ is the tectonic stressing rate (also named tectonic loading rate), supposed unchanged by the stress perturbation, estimated from the slip rate ($\Delta ú$) and the weight and length of the earthquake source (Console et al., 2008):

$$= 32\mu.\Delta ú / \pi^2 (W L)^{1/2} \qquad (5)$$

Where μ is the shear modulus of the elastic medium, and W and L are the width and the length of the fault. Since the Coulomb stress change ΔCFF varies over the surface of the target fault segment, ranging typically from negative to positive values, we take a random value drawn from a distribution computed on the nodes of a regular grid reflecting the spatial pattern on the fault, rather than using the average for the whole fault (e.g., Parsons, 2004). By the modification of the occurrence time due to clock change, Δt, defined in equation (4) we have recalculated the probability of occurrence starting

from January 1, 2013 for a given time period (5-10-30-50 years) for the 26 faults of the Marmara region.

PROBABILITY OF OCCURRENCES FROM ERF MODELS

In fact, one of the main goals of this study has been the computation of the occurrence probability of a characteristic earthquake for the 5-10-30- and 50 year periods (starting from January 1, 2013) on 26 individual seismogenic sources in the Marmara region (Figure 1), considering the uncertainties in the slip rate, characteristic magnitude and aperiodicity of the statistical distribution associated to each examined fault source, by a Monte Carlo technique. Consequently another parameter comes into play is the average recurrence time. The Monte Carlo samples for all these parameters have been drawn from a uniform distribution within their uncertainty limits. The overall uncertainty of the recurrence rates is determined by varying the fault/source parameters simultaneously.

Such probability for each fault was calculated using three earthquake recurrence models: time-independent (Poisson), time-dependent (*BPT*) and time-dependent with inclusion of Δ*CFF* effect (*BPT*+Δ*CFF*) by varying the magnitude and recurrence times verify also in a series of Monte Carlo runs. Then, for each fault segment, among the inter-event time 1000 outcomes, the probability of occurrence was sorted into ascending order, and the 10^{th}, 50^{th} and 90^{th} percentiles were identified. In this computation the parameters coming into play are the uncertainty in the maximum expected magnitude and slip rate. In Figure 2 we give for the three model probability values related to 10^{th}, 50^{th} and 90^{th} percentile of Monte Carlo distribution for the given time intervals.

When we consider the 50^{th} percentile for the next 50 years, according to Poisson and BPT models, we can observe that the largest value of the occurrence probability for the Poisson probability are on the faults Manyas (#20), Cinarcik (#2), West Marmara (#5) and Duzce (#11). While the largest value of the occurrence probability from BPT renewal model may be observed for Cinarcik (#2), Western Marmara (#5) and Bursa (#17) faults (Figure 2)**.**

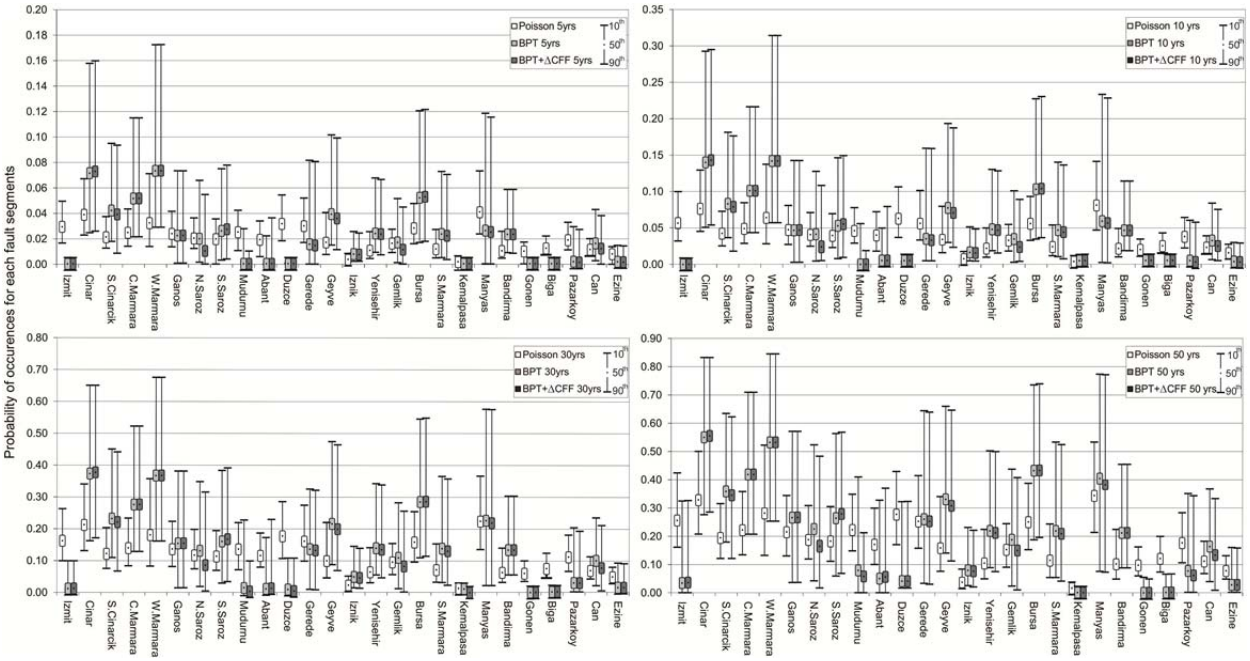

Figure 2. Occurrence probability of a characteristic earthquake e on each fault segment over 5-10-30 and 50 years starting on January 1, 2013 according to Poisson, BPT and BPT+Δ*CFF* with stress inclusion models. For each model the probability values related to 10^{th}, 50^{th} and 90^{th} percentiles are shown in the plot.

EFFECT OF FAULT PARAMETERS ON THE HAZARD MAPS

We have also considered the impact of fault parameter uncertainties (maximum magnitude, and slip rates) on the ground motion hazard for Poisson and BPT forecasting models. Results are presented as

the variability of ground motion by uncertainty maps in the PGA (in units of acceleration, g%) hazard level of 10% exceedance in 50 years (Figure 3a, b, c, and d). We note that in the present study we did not take in to account the ground motion variability caused by the different GMPE choices. In fact only one GMPE model is chosen as defined by AC10 for the active shallow crustal region for assessing the ground shaking hazard in the Marmara region in order to avoid those variability's effect the final seismic hazard estimations in the study region. However, we believe that the uncertainty in the hazard estimates may be reduced significantly by properly modeling the seismic sources and selecting suitable ground motion models and will be the future research in a separate study.

To generate uncertainty maps, the difference between the 50th and 10th percentiles and the 90th and 50th percentiles are selected to indicate the value to be added (Figures 3a and 3c) or subtracted from the hazard map value (Figures 3b and 3d) to obtain the upper and lower limits. As a summary for the maps we can say that the uncertainties are larger around the Izmit (#1), Duzce (#11), Pazarkoy (#24), south Saros (#8), and Manyas (#20) faults area for the time-dependent hazard (around +0.40 g) respect to Poisson case (+0.10 g).

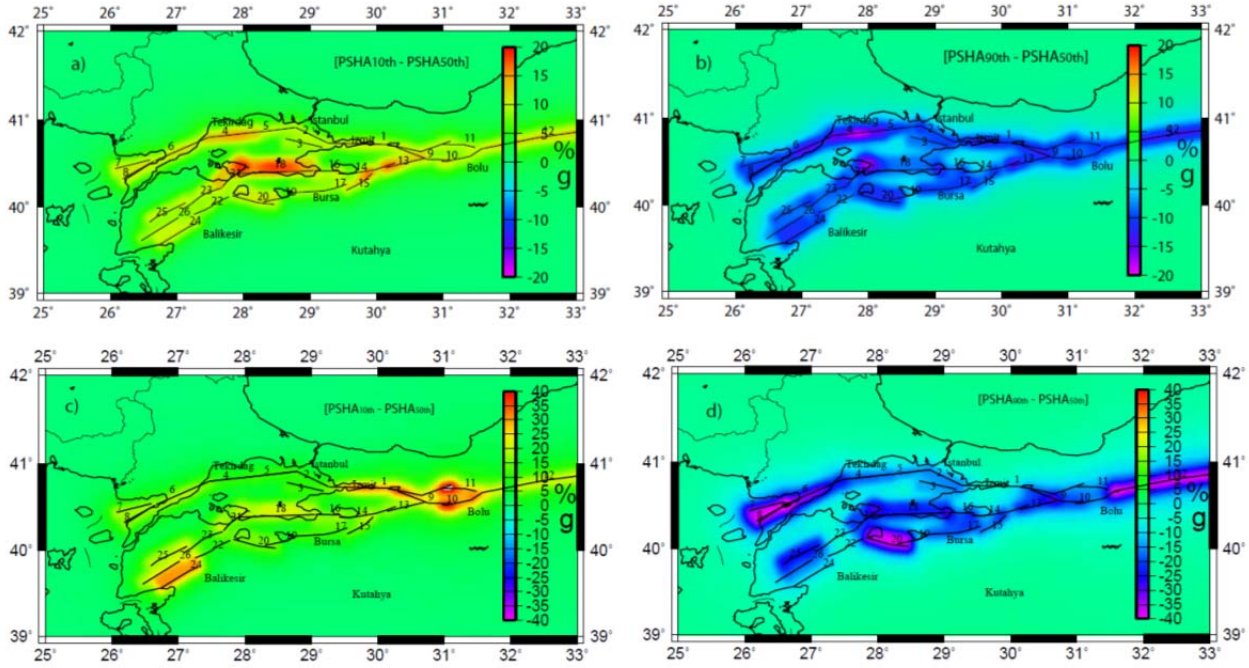

Figure 3. The uncertainty maps in the PGA (in units of acceleration, g%) hazard level of 10% exceedance in 50 years in the Marmara Region; a) the difference between the 50th and 10th percentiles and; b) the difference between the 50th and 90th percentiles, for time-independent Poisson forecasting model; c) the difference between the 50th and 10th percentiles and; d) the difference between the 50th and 90th percentiles, for time-dependent BPT forecasting model.

EFFECT OF PROBABILITY OCCURRENCE MODEL ON THE HAZARD MAPS

The results obtained for the next characteristic earthquake occurrence probability when the uncertainty of the three different earthquake recurrence models is considered, relatively to the 50th percentile of the Monte Carlo distribution, have been the fundamental ingredients for the computation of the PSHA maps of mean PGA on rock having 10% probability of exceedence for the 50 yrs time period starting on January 1, 2013. The comparison among the percentage ratio between the seismic hazards computed by the used three models give us the sensitivity of the ground motion hazard for the earthquake recurrence models.

Figure 4a, b and c show the percentage ratio between the 50th percentile seismic hazards computed with the three models, respectively. It is presented as a relative difference in percentage, computed as:

$$\{[PSHA_{Model1}\text{-}PSHA_{Model2}]/PSHA_{Model2}\} * 100. \qquad (6)$$

The PSHA results based on the time-independent and time-dependent earthquake occurrence models display the effect of the fault recurrence rate and the regency of fault rupture by drastically reducing hazard levels along the eastern part of the NAF zone reaching up to 60-70% nearby Izmit (#1), Duzce (#11), Gonen (#22), Biga (#23) and Pazarkoy (#24) areas. Between models BPT and BPT+Δ*CFF*, the effectiveness of the model choose is lower at the PGA estimation; the increase is up to few percentage and the decrease is up to 20-25%. At SNAF Strands; Pazarkoy (#24), Can (#25) and Ezine (#26) of and the North Saros fault we observed 5% and 10% of decrease in the seismic hazard while this change reaches up to 30-40% around the Izmit and Bolu area due to the negative fault interaction.

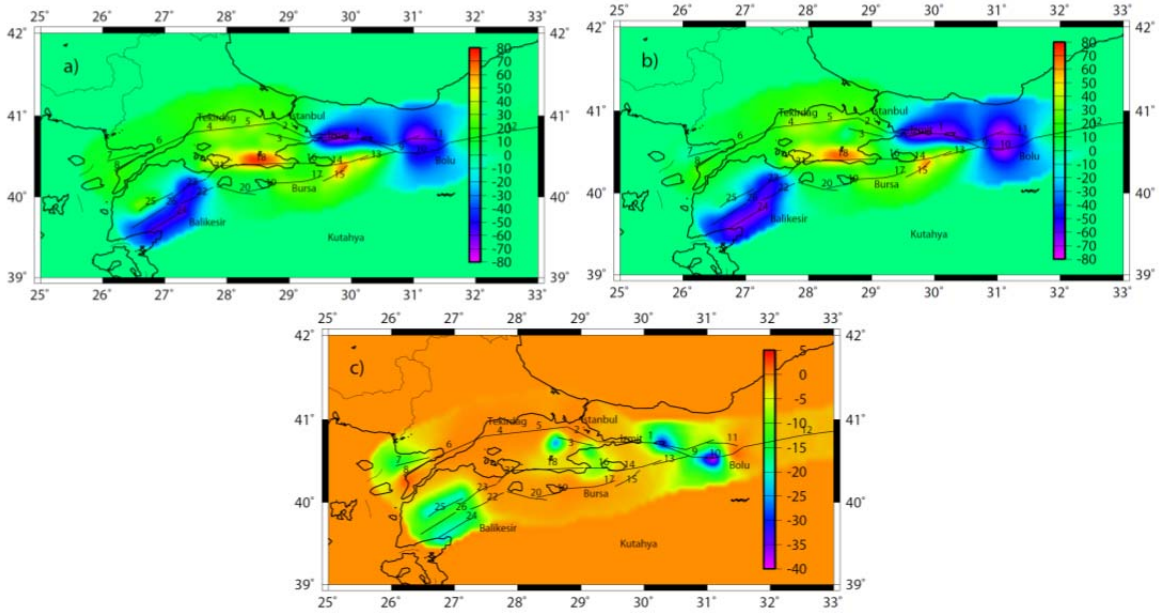

Figure 4. It represents the ratio between the 50th percentiles PGA seismic hazard at a) {[$PSHA_{Poisson}$-$PSHA_{BPT}$]/$PSHA_{BPT}$}*100, *Poisson* and *BPT* (%10 in 50 yrs.), b) {[$PSHA_{Poisson}$-$PSHA_{BPT+\Delta CFF}$]/$PSHA_{BPT+\Delta CFF}$}*100, *Poisson* and *BPT*+Δ*CFF* (%10 in 50 years), c) {[$PSHA_{BPT}$-$PSHA_{BPT+\Delta CFF}$]/$PSHA_{BPT+\Delta CFF}$}*100, *BPT* and *BPT*+Δ*CFF* (%10 in 50 yrs.) calculated using the background seismicity and individual fault segments. In red: positive amplifications. In blue: negative amplifications.

CONCLUSIONS

In this study epistemic uncertainties were considered in the fault-based component of the earthquake rupture forecast. However, epistemic uncertainties were not considered in the parameters (including their spatial correlation) that define the Gutenberg–Richter distribution for background seismicity sources. A methodology for consideration of uncertainties in background source is therefore clearly warranted in order to assess the minimum magnitude and/or *b- value* parameters uncertainty. The future effort will be devoted to defining and quantifying uncertainties in these parameters in a separate study.

Finally, this study is focused on the uncertainties of the parameters of the fault-based component of the earthquake rate forecast and on the earthquake rate forecast methodology itself. We pointed out that the level of complexity in treating time dependent models in the hazard calculations. Therefore, the new maps introduce significant improvements over the previous seismic hazard maps of the region in terms of seismic source characterization, parameterizations and as well as earthquake rate forecasting models. These information are adopted uncertainties on the source parameters is included through a Monte Carlo approach. We estimate the uncertainties of the 10-30- and 50-year probability of occurrence of a characteristic event. Uncertainty on each parameter is represented by the 10th and the 90th percentiles of simulated values.

The choice of fault parameters influences the results of the earthquake rate forecasting models. The geometrical parameters of the fault together with the expected magnitude and long-term slip rate have an influence on the computation of the mean recurrence time, which is the basic ingredient to compute earthquake probability, both under time-independent, Poisson assumption and in time-dependent, renewal approaches. In a few cases we have a T_r larger than the time elapsed. These values have a major influence on the probability of the renewal models.

The results of the present study clearly illustrate the influence of active fault parameters to probabilistic seismic hazard maps. However, the absolute ground-motion levels obtained in this study should be considered with care since these are highly dependent of the assumptions made in the different input parameters and the earthquake rate forecasting models.

We note that in the present study we did not take in to account the ground motion variability caused by the different GMPE choices. In fact only one GMPE model is chosen in order to avoid those variability's effect the final seismic hazard estimations in the study region. However, we believe that the uncertainty in the hazard estimates may be reduced significantly by properly modeling the seismic sources and selecting suitable ground motion models and will be the future research in a separate study.

Since hazard studies are important for their practical implications for society and public policy decision-making processes, an appreciation for the uncertainties and limiting assumptions underlying such studies should be more broadly understood and communicated to the users and decision-making communities. These maps are useful as long as their limitations are recognized. The uncertainty analysis can suggest future research to resolve some of the important questions that affect earthquake occurrence probabilities and ground shaking hazard.

REFERENCES

Akkar S and Cagnan Z (2010). A local ground-motion predictive model for Turkey and its comparison with other regional and global ground-motion models. *Bull. Seism. Soc. Am.* 100, 2978–2995.

An, LY (1997). Maximum link distance between strike–slip faults: observations and constraints. *Pure Appl. Geophys.* 150, 19–36.

Armijo R, Pondard NMeyer, B Mercier de Lepinay, B Ucarkus, G Malavieille, J Dominguez, S, Gustcher, M-A Beck, Çagatay N Cakir Z, Imren, C, Kadir E and Natalin, and MARMARA SCARPS cruise party, (2005). Submarine fault scarps in the Sea of Marmara pull-apart (North Anatolian Fault): Implications for seismic hazard in Istanbul, *Geochem. Geophys. Geosyst.*, 6, Q06009, doi:10.1029/2004GC000896.

Atakan K, Ojeda A, Meghraoui M, Barka A, Erdik M, Bodare A., (2002) Seismic Hazard in Istanbul following the 17 August 1999 Izmit and 12 November 1999 Düzce earthquakes. Bull Seism Soc Am 92:466–482.

Barka A, Kadinsky-Cade K (1998). Strike-slip fault geometry in Turkey and its influence on earthquake activity, *Tectonics*, 7, 663–684, doi:10.1029/TC007i003p00663.

Console R, Murru M, Falcone G and Catalli F (2008). Stress interaction effect on the occurrence probability of characteristic earthquakes in Central Apennines, *J. Geophys. Res.*, 113, B08313, doi:10.1029/2007JB005418.

Console R, Falcone G, Karakostas V, Murru M, Papadimitriou E, Rhoades D (2013). Renewal models and co-seismic stress transfer in the Corinth Gulf, Greece, fault system, *J. Geophys. Res*., 118, 1-119, doi:10.1002/jgrb.50277.

Cramer, CH, Petersen MD, Cao T, Toppozada TR, Reichle M (2000). A time dependent probabilistic seismic-hazard model for California, *Bull. Seism. Soc. Am.,* 90 (1), 1-21.

Ellsworth WL, Matthews MV, Nadeau RM, Nishenko SP, Reasenberg PA, Simpson RW (1999). A physically-based earthquake recurrence model for estimation of long-term earthquake probabilities, *Open-File Rep*, *U.S. Geol. Surv*., 99-522, p.23.

Erdik M, Demircioglu M, Sesetyan K, Durukal E, Siyahi B (2004). Earthquake hazard in Marmara Region, Turkey, *Soil Dynamics and Earthquake Engineering,* 24, 605-631.

Field EH, Jackson DD and JF Dolan (1999). A mutually consistent seismic-hazard source model for Southern California, *Bull. Seism. Soc. Am*., 89, 3, 559-578.

Gulerce Z and S Ocak (2013). Probabilistic seismic hazard assessment of Eastern Marmara Region, Bulletin of Earthquake Engineering, 11 (5), 1259-1277.

Harris, RA, and Day SM (1999). Dynamic 3D simulations of earthquakes on en echelon faults. *Geophys. Res. Lett.* 18, 893–896.

Harris R.A, and RW Simpson (1998). Suppression of large earthquakes by stress shadows: A comparison of Coulomb and rate and state failure, *J. Geophys. Res.,* 103, 439–451, 1998.

Kalkan E, Gülkan P, Yilmaz N, Çelebi M (2009). Reassessment of probabilistic seismic hazard in the Marmara Region. *Bull Seism Soc Am.* 99(4):2127–2146.

Kase Y and Kuge K (2001). Rupture propagation beyond fault discontinuities: significance of fault strike and location. *Geophys. J. Int.* 147, 330–342.

King GCP, Stein RS and Lin J (1994). Static stress changes and the triggering of earthquakes, *Bull. Seismol. Soc. Am.*, 84, 935–953.

Lettis W, Bachhuber J, Witter R, Brankman C, Randolph CE, Barka A, Page WD, Kaya A (2002). Influence of releasing stepovers on surface fault rupture and fault segmentation: examples from the 17 August 1999 Izmit earthquake on the North Anatolian Fault, Turkey. *Seism. Soc. Am. Bull*. 92 (1), 19–42.

Matthews MV, Ellsworth WL, Reasenberg PA (2002). A Brownian model for recurrent earthquakes, *Bull. Seismol. Soc. Am.,* **92**, 2233–2250.

Parson T, Toda S, Stein RS, Barka A, Dietrich JH (2000). Heightened odds of large earthquakes near Istanbul: an interaction-based probability calculation, *Science*, **288**, 661-665.

Parsons T (2004). Recalculated probability of M ≥ 7 earthquakes beneath the Sea of Marmara, Turkey, *J. Geophys. Res*., 109, doi:10.1029/2001JB002667.

Pondard N, Armijo R, King GCP, Meyer B, Flerit F (2007). Fault interactions in the Sea of Marmara pull-apart (North Anatolian Fault): earthquake clustering and propagating earthquake sequences, *Geophys. J. Int.*, 171.

Segall P and DD Pollard (1980). Mechanics of discontinuous faults, *J. Geophys. Res*., 85, 4337 – 4350.

Sibson RH (1985). Stopping of earthquake ruptures at dilational fault jogs. *Nature* 316, 248–251.

Wells DL, and Coppersmith KJ (1994). New empirical relationships among magnitude, rupture length, rupture width, rupture area, and surface displacement. *Bull. Seismol. Soc. Am.* 84(4), 974–1002.

Wesnousky SG (1988). Seismological and structural evolution of strike–slip faults. *Nature* 335, 340–343.

Wesnousky SG (1994).The Gutenberg-Richter or characteristic earthquake distribution, which is it?*, Bull. Seismol. Soc. Am.,* 84, 1940-1959.